Studies of the Binding and Structure of Adrenocorticotropin Peptides in Membrane Mimics by NMR Spectroscopy and Pulsed-Field Gradient Diffusion

Xinfeng Gao and Tuck C. Wong
Department of Chemistry, University of Missouri, Columbia, Missouri 65211

ABSTRACT The partition and structure of three adrenocorticotropic hormone peptides ACTH(1–10), ACTH(1–24), and ACTH(11–24) in water and in sodium dodecylsulfate (SDS) and dodecylphosphocholine (DPC) micelles were studied by 2D NMR and NMR gradient diffusion measurements. The diffusion rates, the NH chemical shifts, and the nuclear Overhauser effect patterns provided a coherent picture of binding of these peptides. All three peptides are significantly partitioned in the negatively charged SDS micelles and possess definite secondary structure, as opposed to random structures in water. For ACTH (1–24), the hydrophobic 1–10 segment is partitioned in DPC micelles, but the charged 11–24 segment prefers to remain in the aqueous region. ACTH(11–24) does not bind significantly to the DPC micelles. The binding of the ACTH peptides in these two widely used "membrane mimics" are substantially different from that in 1-palmitoyl-2-oleoyl-sn-glycero-3-phosphocholine (POPC) bilayers obtained by attenuated total reflection infrared spectroscopy and from our preliminary diffusion studies of the same peptides in POPC vesicles. This study showed that, in a given micellar medium, all corresponding segments of these peptides are located in the same membrane environment in the system, regardless of whether these segments exist by themselves or are attached to other segments. This result may contradict the membrane-compartments concept of Schwyzer, which suggests that ACTH(1–10) and ACTH(1–24) are located in different membrane compartments because they have different address segments, and consequently, bind to different receptors. The present results also suggest that the assumption that micelles are good membrane mimics should be carefully examined.

INTRODUCTION

Adrenocorticotropin hormone (ACTH) is a 39-residue peptide found in the anterior lobe of the pituitary gland and in certain regions of the brain (Schwyzer, 1977). Several N-terminal segments of ACTH are found to have hormonal activities and specific receptor-binding properties. ACTH (1–24) binds to steroidogenic receptors, whereas ACTH (1–10) is found to bind preferentially to central nervous receptors. The fragment ACTH (11–24) is an antagonist for steroidogenesis without any agonist properties. It was concluded that segment 1–10 of ACTH (1–24) carries the message for triggering responses from the receptors, and the segment 11–24 (the address segment) modulates the potency of the message segment with different receptors (Schwyzer, 1977).

Few NMR studies of ACTH peptide fragments have been reported. For example, ACTH (1–10) has been studied in solution (Rawson et al., 1982; Tunga and Hosur, 1992). Proton NMR (Toma et al., 1978) of ACTH (1–32), ACTH (1–24), and several C-terminal fragments showed the existence of the *trans-cis* isomerism involving Pro^{24}. The fraction of the *cis*-Pro^{24} isomer in these peptides ranges from 22% to ~50% for ACTH(1–24) in water. ^{13}C assignment of several ACTH fragments was also made, and the existence of the *trans-cis* isomerism of Pro^{24} corroborated (Toma et al., 1981). Recently, in a preliminary report on the ^{15}N labeling of ACTH (1–24) (Uegaki et al., 1996), it was shown via the ^{15}N-^{1}H heteronuclear single-quantum coherence (HSQC) signals (Bax et al., 1990) that there are multiple isomeric forms at the C-terminus of the peptide. No assignment of the HSQC signals was presented, however. The interaction of these three peptides with lipid bilayers has been studied by attenuated total reflection infrared (ATR-IR) spectroscopy and by hydrophobic photolabeling (Gysin and Schwyzer, 1984; Gremlich et al., 1983, 1984).

In this work, the complete ^{1}H NMR chemical shift assignments of ACTH (1–24) (Ser-Tyr-Ser-Met-Glu-His-Phe-Arg-Trp-Gly-Lys-Pro-Val-Gly-Lys-Lys-Arg-Arg-Pro-Val-Lys-Val-Tyr-Pro-OH), ACTH (1–10), and ACTH (11–24) in water, in sodium dodecylsulfate (SDS), and in dodecylphosphocholine (DPC) micelles have been obtained. These two micellar media are the most frequently used "membrane mimics" in high-resolution NMR. The binding of the ACTH peptide fragments to these two micelles was studied by pulsed-field-gradient diffusion methods (Stilbs, 1987). The secondary structures of these peptides in the micellar system have also been determined. The binding and the secondary structure of these peptides in micelles are compared with each other, as well as with those of the same peptides in lipid bilayers as determined by ATR-IR (Gysin and Schwyzer, 1984; Gremlich et al., 1983, 1984). One of the main goals of this work is to determine whether the binding of these ACTH peptides to these micelles and the induced secondary structure upon binding are similar to their binding to lipid bilayers, thus examining the validity of

Received for publication 13 March 1997 and in final form 9 December 1997.

Address reprint requests to Dr. Tuck C. Wong, Department of Chemistry, University of Missouri, Columbia, MO 65211. Tel.: 573-882-7725; Fax: 573-882-2754; E-mail: chem1060@showme.missouri.edu.

0006-3495/98/04/1871/18 $2.00

the widely held assumption that these micelles are good membrane mimics.

EXPERIMENTAL PROCEDURES

Samples

The ACTH peptides were obtained from the American Peptide Company (Sunnyvale, CA) and from Sigma Biochemicals (St. Louis, MO). All peptides are of >95% purity and were used without further purification. SDS-d_{25} was purchased from Cambridge Isotopes, and DPC-d_{38} was purchased from two sources, Cambridge Isotopes and Avanti Polar Lipids (Alabaster, AL). The diffusional properties of DPC from these two sources were shown in this work to be identical. 1-Palmitoyl-2-oleoyl-sn-glycero-3-phosphocholine (POPC) was purchased from Avanti Polar Lipids. A typical sample was made of 1 mg of peptide in 0.3 ml of solvent in a 5-mm Shigemi NMR tube, corresponding to 2–4 mM in peptide concentration. For aqueous samples, 85% H_2O/15% D_2O was used. For the micellar samples, the solution was made of 42 mM SDS-d_{25} or 98 mM DPC-d_{38} in 85% H_2O/15% D_2O. The concentrations of these two surfactants/lipids are sufficiently high compared with their respective critical micelle concentrations (8 mM for SDS and 1 mM for DPC) to ensure the predominance of micellar aggregates. The concentration is also high enough to fall into the region where the peptide chemical shifts no longer change with changing peptide/micelle ratio (Lauterwein et al., 1979; Kallick, 1995). For diffusion measurement purposes, a small amount of hexamethyldisilane (HMDS) (Aldrich, Milwaukee, WI) was added to the micellar samples as a probe for measuring the diffusion of the whole micelle.

The pH of the aqueous samples was adjusted to 7.5 ± 0.1 by adding a small amount of NaOH or HCl. The pH of SDS samples was 7.6 for all samples without adjustment. For DPC samples, the pH was 5.8 ± 0.2.

The procedure for preparing small unilamellar vesicles followed that described by Barenholz et al. (1977). The buffer used was 50 mM potassium phosphate in 0.1 M NaCl. NaOH was added to adjust the pH to 6.8–7.2. Except for the stepwise titration experiment involving ACTH (1–24) described in a later section, the POPC concentration was 132 mM. An equal volume of peptide solution of ~1 mg/ml was titrated into the vesicle solution, resulting in a final POPC concentration of 66 mM. The peptide/vesicle mixture was adequately stirred before being used for NMR experiments.

NMR spectroscopy

All NMR experiments were performed on a Bruker DRX-500 MHz spectrometer. For diffusion measurements, the gradient strength used is ~50 G/cm for each axis and was calibrated by the known diffusion coefficient of water (Mills, 1973). For most of the samples, the following experiments were done: one-dimensional ^{1}H spectra, total correlation spectroscopy (TOCSY) spectra (Davis and Bax, 1985; Griesinger et al., 1988), and nuclear Overhauser effect spectroscopy (NOESY) spectra (Jeener et al., 1979; Kumar et al., 1980). For peptides in aqueous solution, rotating frame nuclear Overhauser effect spectroscopy (ROESY) spectra (Bax and Davis, 1985) were also obtained in addition to NOESY spectra. For some samples, a double-quantum-filtered correlation spectroscopy (DQF-COSY) spectrum (Shaka and Freeman, 1983) was also obtained. The typical experimental conditions for all two-dimensional NMR experiments were as follows. The ^{1}H 90° pulse was ~8 μs. All experiments were obtained in the phase-sensitive mode by using the time proportional phase increment method (Bodenhausen et al., 1984). Typically 16–32 scans per t_1 were acquired in 512 × 2K data sets, which were then zero-filled to 1K × 2K after Fourier transform in both dimensions. π/3-shifted sine-bell squared apodization was used in both dimensions. Water suppression was achieved by using WATERGATE (Sklenar et al., 1993) in all 2D experiments. In 1D experiments, either WATERGATE or low-power presaturation was used. The TOCSY mixing time was 75–100 ms, and several NOESY mixing times were used for micellar samples: 50, 100, 200, and 250 ms. For aqueous samples, a single NOESY mixing time of 200 ms was used.

For diffusion experiments, the pulsed field-gradient stimulated echo (PFG-STE) pulse sequence (Tanner, 1970) was used. The diffusion time (Δ) was usually 50 ms, and the gradient duration (δ) was 5 ms. The relaxation delay was 10 s. Sixteen to thirty-two scans were obtained for each spectrum. The PFG was applied in both the x and y directions for micellar samples, and only in one of these axes for aqueous samples. The gradient strength in a series of experiments was incremented from 0.5 G/cm to ~50 G/cm, usually in 10–13 steps. The decay of the signal usually covered two decades. A typical set of data from the diffusion experiment for the peptide/micelle system is shown in Fig. 1, where the diffusion coefficients for both the peptide (ACTH (1–10)) and the DPC micelles can be measured simultaneously. The diffusion coefficient was determined from the diffusion data with Bruker XWINNMR software, and the exponentiality of the decay was checked in each case.

Experiments were usually performed at 298 K. For some samples, other temperatures ranging from 278 K to 313 K were also used. The temperature was controlled by passing dried air over the probe through a Haake constant temperature bath. The stability of the temperature control was better than 0.1°K.

Determination of peptide partition from diffusion measurements

The determination of the partition coefficient of the peptides in micelles by NMR diffusion techniques is similar to the work of Stilbs, in the measurement of partition (or solubilization) of small molecules in micelles (Stilbs, 1982).

In a PFG-STE experiment, the NMR signals derived from the stimulated echo are given by

$$I = \sum_i I_{oi} \exp[-D_i K^2(\Delta - \delta/3)] \qquad (1)$$

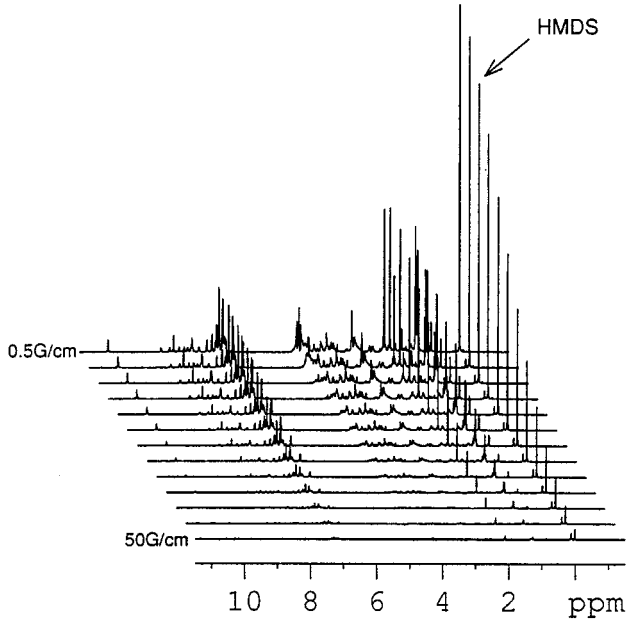

FIGURE 1 The decay of the ACTH (1–10) and DPC (98 mM) signals in a STE-PFG experiment at 298 K. During the experiment, the duration of the gradient pulses, δ (5 ms), and the diffusion time, Δ (50 ms), were kept constant, while the strength of the gradient pulses (in both the x and y directions), g, was incremented from 0.5 G/cm to 50 G/cm in 13 steps. The signal at ~0 ppm was that of HMDS, which was used to monitor the diffusion of the DPC micelles. The peptide signals, particularly the aromatic signals between 6 and 7.2 ppm, were used to determine the diffusion coefficient of the peptide.

where I and I_o are the intensities from the STE pulse sequence with and without the PFG, respectively. $K = \gamma\delta g$, where γ is the magnetogyric ratio of the nucleus, and δ and g are the gradient duration and strength, respectively. Δ is the duration between the gradient pulses (the diffusion time), and D_i is the diffusion coefficient of the ith species or the ith signal in the sample. The decay of the PFG echo is usually exponential for micellar systems (according to Eq. 1), because of either the monodispersity of the micellar size or the fast exchange of monomers between micelles (Stilbs, 1987; Morris et al., 1994). This has also been verified in all of the peptide/micelle samples in this work.

The analysis of the peptide diffusion data in the SDS and in DPC micelles will be based on the two-site model, which is applicable when the exchange between the peptides in free form and peptides solubilized in the micelles is fast compared to the pertinent NMR time scale. Thus the measured diffusion coefficient, D_{obs}, obtained from the decay of the peptide signals (Eq. 1) is given by (Stilbs, 1983, 1987)

$$D_{obs} = f_b D_b + (1 - f_b) D_f \quad (2)$$

where D_f and D_b denote the diffusion coefficients of the peptide in the free and bound (partitioned) forms, respectively; f_b is the fraction of the bound peptides. Because the root mean square displacement of the peptide during the diffusion time allowed in the experiment (typically ~50 ms) is much larger than the dimension of the micelles, D_b can be taken as equal to the diffusion coefficient of the micelles, D_{mic}.

D_{mic} can be measured with the PFG-STE experiment from the signals of the SDS (or DPC) directly, or more accurately and conveniently from the signal of a small amount of a hydrophobic probe molecule, which is known to be completely partitioned within the hydrophobic core of the micelles. Because of the effects of the monomer-micelle exchange, the apparent diffusion coefficient obtained directly from surfactant/lipid signals is usually from 5% to 10% higher than the actual D_{mic} determined from the diffusion of the probe molecule, depending on the concentration of the micelle versus the critical micelle concentration of the micelle. Moreover, because perdeuterated SDS and DPC are used for the peptide/micelle systems for NMR studies, it is necessary to measure D_{mic} via the probe molecules. Hexamethyldisilane (HMDS) has been widely used as the probe molecule for this purpose in diffusion studies of micellar systems (Stilbs, 1987) and has been verified to be applicable to both SDS and DPC micelles in this work. D_f will be obtained from the following expression for small molecules obstructed by spherical particles, micelles in this case (Jonsson et al., 1986),

$$D_f = D_f^o/(1 + \phi/2) \quad (3)$$

where D_f^o is the diffusion coefficient of free peptides in water and will be measured for peptides in water samples of the same concentration and temperature, and ϕ is the volume fraction of the obstructing particles (micelles), which is usually approximated by using the weight fraction of the micelle-forming component (Jonsson et al., 1986). The potential effects of peptide aggregation on D_f^o were determined by measuring the diffusion coefficient of free peptide in successively diluted samples down to a practical lower concentration limit (~0.1–0.3 mM, depending on samples). From the calculation of f_b (Eq. 2) derived from the various measured diffusion coefficients, the partition coefficient of the peptides in micelles, p, defined as

$$p = [P]_{micelle}/[P]_{aqueous} \quad (4)$$

where [P] is the peptide concentration in the respective phases (assuming the activity coefficients are unity), can be determined. The partition coefficient is related to f_b by the following:

$$[P]_{micelle} = n_p \times f_b/V_{micelle} \quad (5)$$

$$[P]_{aqueous} = n_p \times (1 - f_b)/V_{aqueous} \quad (6)$$

where n_p is the total number of moles of peptide in the sample; $V_{micelle}$ and $V_{aqueous}$ are the phase volumes of the micelles and the aqueous bulk, respectively; and their ratio is approximated by their respective weight fractions, or by using the partial molal volume (Brun et al., 1978) or the partial specific volume (Lauterwein et al., 1979) of the micelles if the latter are known. From the partial molal volumes determined for SDS, several tetramethylammonium laurates, and DPC, it can be concluded that these two ways of estimation of the $V_{micelle}$ usually differ by less than 10%. For the purpose of estimating the free energy of partitioning, the errors introduced are ~1%, which is within the current level of experimental error, and is consistent with errors from other experimental methods for the free energy of partition in lipid bilayers (Beschiaschvili and Seelig, 1992; Seelig et al., 1993).

RESULTS

Partitioning in SDS and DPC micelles

The partition of the ACTH fragments (1–24, 1–10, and 11–24) were measured in both SDS and DPC micelles by pulsed-field gradient diffusion techniques. The $D_{peptide}$ was determined from the average of several (typically 5–10) peptide signals (for peptide chemical shift assignments, see next section), and the deviation of the individual diffusion coefficient from the average is usually within ±1%. $D_{micelle}$ was determined from that of the HMDS signal. As shown in Table 1, the partition of all ACTH peptide fragments in 42 mM SDS micelles is close to 100%, yielding partition coefficients of $>5 \times 10^3$.

For the zwitterionic DPC, the pattern is quite different. The partitions of ACTH (1–10) and (1–24) are also close to 100%. However, for the highly charged ACTH (11–24), the partition (23%) is substantially lower than the other fragments containing hydrophobic segments (the 1–10 and 1–24 fragments), yielding a partition coefficient ~150 times lower than that of the 1–10 and 1–24 segments. The differ-

TABLE 1 The partition, f_b (in %, ± 0.5%) and the partition coefficient, p*, of ACTH peptide fragments in SDS and DPC micelles and in phosphocholine bilayers

	ACTH (1–10)		ACTH (11–24)		ACTH (1–24)		
	f_b	p	f_b	p	f_b	p	Ref.
SDS micelle	99.5	1.4×10^4	100	$>3.7 \times 10^5$	98.6	4.9×10^3	This work
DPC micelle	98.0	$1.1 (\pm 0.14) \times 10^3$	23.4	7.3 ± 0.1	97.9	$1.1 (\pm 0.14) \times 10^3$	This work
POPC bilayer and vesicles	No binding		Low surface binding		High insertion		#

*The uncertainties in the determination of p depends on the value of f_b. Since the partition coefficient is calculated from $f_b/(1 - f_b)$, the uncertainty is very large when f_b is close to 100%. Thus the probable value of p for ACTH (1–10) in SDS is $1.0 - 2.3 \times 10^4$; and $4.3 - 5.8 \times 10^3$ for ACTH (1–24) in SDS.
#Gremlich et al. (1983, 1984), Gysin and Schwyzer (1984).

ence between the rate of diffusion of ACTH (11–24), and ACTH (1–10) and ACTH (1–24) in 98 mM DPC is quite obvious, even by visual inspection. The signals of ACTH (11–24) decayed (with respect to $K^2(\Delta\text{-}\delta/3)$) significantly faster than that of the micelle (probe) signal, whereas the signals of ACTH (1–24) and ACTH (1–10) decayed at almost the same rate as that of the micelle (probe) signal (Fig. 1), indicating that the latter are almost completely bound to (or partitioned in) the micelles. The observed diffusion coefficient for ACTH (11–24) is 1.76×10^{-10} m^2/s at 298 K, whereas that of ACTH (1–10) is 8.61×10^{-11} m^2/s, and 7.72×10^{-11} m^2/s for ACTH (1–24) under the same conditions. The twofold difference in the observed diffusion coefficient reflects the large difference in the partitioning of these peptides in the DPC micelles (Eq. 1). Thus the result suggests that the primary interaction of the DPC micelles with these peptides is the hydrophobic interaction, whereas the highly charged peptide ACTH (11–24) prefers to remain in the aqueous phase. This conclusion is corroborated by the chemical shifts and the secondary structures, which will be presented in a later section.

The concentration dependence of the diffusion coefficient of the ACTH peptides in water was measured to ascertain that no significant aggregation of the peptides occurred in the concentration range being used. Measurements of the diffusion coefficient of the peptides were made of samples successively diluted from ~2 mM to 0.25 mM (the exact concentration differed slightly for different peptides). No significant variation or trend in the diffusion coefficients was observed with the concentration change, indicating that the aggregation effect on the measured diffusion coefficients of the ACTH peptides is not significant.

The diffusion coefficients of the micelles and of the peptide/micelle complexes as measured from the HMDS probe molecules in the pure micelles and in micelle/peptide samples also provided information on the aggregation number and hydrodynamic radius of these aggregates, which are quite similar to those determined by Lauterwein et al. by sedimentation and by light scattering (Lauterwein et al., 1979). The aggregation number of ~56 was determined in Lauterwein's study by diffusion and by using analytical ultracentrifugation, from which the weight of the micelles was measured (Lauterwein et al., 1979). Because the diffusion coefficient for the DPC micelles determined in this study is essentially the same as that determined in Lauterwein's work, the aggregation number was thus ~56 as well. However, the diffusion coefficients measured by Kallick et al. by NMR diffusion (Kallick et al., 1995) were substantially lower, after correcting for the difference in the temperature at which the measurements were made (310 K in Kallick's work versus 298 K in this study). The radius of the DPC micelles, after correction for ~6 Å of the maximum thickness of the hydration shell, is 22.2 Å for the 98 mM DPC micelles. Similarly, for SDS micelles, the diffusion coefficients measured for 42 mM and 108 mM micelles showed the expected increase in the hydrodynamic radius of the SDS micelles with increasing surfactant concentration. The aggregation numbers of the SDS micelles of ~60 (Croonen et al., 1983) at 42 mM and a radius (after correction of the hydration shell) of 22.8 Å are consistent with previous determinations by x-ray scattering (Itri and Amaral, 1991) and by NMR relaxation (Soderman et al., 1988). Incorporation of the peptide into the micelles decreases the diffusion coefficient of the micelles, leading to an apparent increase in the hydrodynamic radius. Thus the apparent hydrodynamics radius (not corrected for the hydration shell) falls in the range of 29.2–31.7 Å for DPC and 30.1–37.7 Å for SDS micelles after the incorporation of the ACTH peptides, assuming that the micelles remain close to spherical. There is no major change in the aggregation number upon binding of the peptide.

Partitioning in POPC vesicles

The diffusion coefficient of the POPC vesicles ranged from 1.8 to 2.2×10^{-11} m^2/s in several different preparations, corresponding to a diameter of the vesicles in the 20–28 nm range, which falls in the range expected for small unilamellar vesicles. The existence of separate inner and outer choline $N(CH_3)^+$ methyl signals at ~3.2 ppm also provided positive evidence for the formation of vesicles (Bystrov et al., 1971). The diffusion results of the peptide in the presence of the vesicles showed that the partition of ACTH (1–10) in the POPC vesicles is substantially lower than in either of the micelles. The fraction of ACTH (1–10) in the 66 mM POPC vesicles is less than 10%, corresponding to a partition coefficient of ~1.6, which is about three to four orders of magnitude lower than that in DPC and SDS micelles, respectively (Table 1).

For ACTH (1–24), the observed diffusion coefficient of the peptide in the presence of POPC vesicles is almost identical to that of the free peptide in water. The small reduction in the diffusion coefficient can be accounted for completely by the obstruction effect of the vesicles (Eq. 3). The cause of this seemingly unexpected result was investigated by a stepwise titration of an aqueous ACTH (1–24) sample with concentrated POPC (260 mM) solution. A gradual loss of the ACTH signals upon the addition of POPC was observed. The reduction of peptide signals was corrected for the dilution effect, which was monitored by the change of the intensity of the signal of sodium 3-trimethylsilylproprionate-2,2,3,3-d_4 (deuterated TSP). It is thus concluded that the reduction of the peptide signals was due to the severe broadening (and loss) of the signals of the peptide partitioned into the vesicles. Furthermore, the exchange between the partitioned and the free peptides is slow in the NMR time scale, and thus the assumption employed in Eq. 2 is no longer valid. The measured diffusion coefficient of the peptide based on the free peptide signals thus represents solely that of the free peptide. The fraction of partitioned ACTH (1–24) in POPC is higher than that of ACTH (1–10) described above. At the same final vesicle concentration, the partition of ACTH (1–24) is at least five

times higher than that of ACTH (1–10). The quantitative results on ACTH (1–24) have not been completely determined, and the complete results, including the temperature dependence of partition, will be presented elsewhere. However, the qualitative results that ACTH (1–24) has a higher partition in POPC vesicles than ACTH (1–10), and that the exchange of the former between the free and partitioned states is much slower than that of the latter, indicating a stronger interaction with the bilayers, are in essential agreement with the results of Schwyzer et al. for ACTH peptides in POPC bilayers and vesicles (Gysin and Schwyzer, 1984; Gremlich et al., 1983, 1984). In addition, similar results for ACTH (1–24) were obtained in this work, regardless of whether 0.1 M NaCl was present in the buffer used in preparing the vesicles.

Chemical shift assignments

The chemical shift assignments of all ACTH fragments in the various media were made by using TOCSY primarily to identify the spin systems of the residues, and by using NOESY and/or ROESY to establish the sequential assignments. The complete ^{1}H chemical shift assignments are given in Tables 1a, 1b, and 1c.

Trans-cis isomerism at Pro^{12}, Pro^{19}, and Pro^{24}

Complications arose for ACTH (1–24) and ACTH (11–24) where more than one set of signals for the residues at the C-terminus were observed. For both peptides, two strong sets of NH and αH signals for residues between Pro^{19} and Pro^{24} can be clearly assigned. This is consistent with the results of previous studies of Toma et al. (1978, 1981), that *cis* and *trans* isomers of Pro^{24} exist for the C-terminal fragments of ACTH in water. However, in this study, we have found that *cis-trans* isomerism occurs at all three proline sites, with varying ratios of the *cis/trans* isomers, depending on the site as well as on the medium. Fig. 2 shows the αH-δH region in the NOESY map of ACTH (11–24) in 42 mM SDS, which contains the α-α correlations for Tyr^{23}-Pro^{24} (strong) and for Arg^{18}-Pro^{19} and Lys^{11}-Pro^{12} (weaker). The presence of the α-α correlations indicates the presence of the *cis* isomers for all three prolines. The results can be summarized briefly as follows.

1. *Trans-cis* isomerism is most significant at Pro^{24}. For Pro^{19} and Pro^{12}, *trans-cis* isomerism is more significant in SDS micelles than in DPC micelles and in water.

2. The *cis-trans* isomer ratios for all three Pro sites are medium-dependent. The fraction of *cis* isomers ranges from 42% (uncertainties $\pm$ 2%) for *cis*-Pro^{24} in SDS micelles to only ~8% for *cis*-Pro^{12} and *cis*-Pro^{19} in DPC micelles. The ratios in SDS micelles differ from those in DPC micelles and in water. The ratios are identical to within experimental uncertainties in the latter two media. Because all three prolines exist in the 11–24 segment, this is an indication that the 11–24 segment exists in a similar environment in both water and in DPC micelles, but in a different environment in SDS micelles. This inference is corroborated by the binding, chemical shift, and NOE results (see Discussion section).

A complete chemical shift assignment of all of the stereoisomers is very complicated, especially in SDS, where there are, in principle, eight isomeric forms for the 11–24 segment. This task is beyond the scope of this work, and it is not central to the main conclusions of this work. Therefore, only the chemical shift assignments of the two main isomeric forms, *trans*- and *cis*-Pro^{24} (with both Pro^{12} and Pro^{19} in the *trans* form), and their NOEs (see tables) are presented and discussed. Detailed chemical shift assignments, determination of *cis-trans* isomer ratios, and the discussion on the solvent effects on the *cis-trans* equilibrium will be presented elsewhere.

Linewidths

In analyzing the respective 1D and 2D spectra, we observed differences in linewidths between samples. All samples in SDS micelles exhibited by far the largest linewidths. In contrast, samples in DPC suffered only mildly from the line-broadening (as compared with the corresponding aqueous samples) problems. The difference in the linewidths in these two micelles may arise from two factors: 1) the higher degree of partitioning of the peptides in SDS micelles than in DPC micelles, and 2) the peptides may interact with the headgroup of SDS more strongly, resulting in more restriction in the motion of the peptides with respect to the micelles. The linewidths of ACTH (11–24) in DPC are particularly narrow, indicating a low degree of partitioning in the DPC micelles, which is consistent with the partition results discussed above. In the case of ACTH (1–24) in DPC micelles, a rather striking contrast between the linewidths of residues 1–10 and residues 11–24 was observed. The former were broadened as ACTH (1–10) in DPC, whereas the linewidths of the 11–24 residues were much narrower. The difference in the linewidths clearly manifested itself in the TOCSY signals. Because of the shorter transverse relaxation time (T_2) of the signals for the 1–10 residues, which causes faster decay of the signals during the Hartman-Hahn mixing period, the TOCSY correlations are much weaker for signals from the 1–10 segment than those from the 11–24 segment, and many long-range correlation peaks (such as NH-βH and NH-γH) for the 1–10 residues vanished (Fig. 3). A rather striking difference can be found by comparing the vastly different intensities of the TOCSY signals of Gly^{10} and Gly^{14} (Fig. 3). This striking difference in T_2 between the hydrophobic (1–10) segment and the charged (11–24) segment is a strong indication that the two segments have very different motional characteristics, because of different degrees of interaction with the DPC micelles. The 1–10 segment is partitioned in the micelles and is more restricted in its motions, whereas the 11–24 segment protrudes into the aqueous phase and is less restricted in its motions, leading to a much longer T_2. The difference in T_2 can be appropriately described in terms of

TABLE 1a ^{1}H chemical shift assignment (in ppm) for ACTH(1–10), ACTH(11–24), and ACTH(1–24) in H_2O at 298 K

Residue		ACTH(1–10)	ACTH(11–24)				ACTH(1–24)			
			Pro^{24}	(*trans*)	Pro^{24}	(*cis*)	Pro^{24}	(*trans*)	Pro^{24}	(*cis*)
Ser^1	NH									
	α-CH	4.19						4.18		
	β-CH	4.04, 4.04						4.02, 4.02		
Tyr^2	NH	8.78						8.78		
	α-CH	4.73						4.70		
	β-CH	3.11, 3.05						3.06, 3.06		
	2,6H	7.19						7.16		
	3,5H	6.89						6.86		
Ser^3	NH	8.41						8.40		
	α-CH	4.47						4.43		
	β-CH	3.94, 3.86						3.90, 3.83		
Met^4	NH	8.40						8.39		
	α-CH	4.50						4.48		
	β-CH	2.16, 2.05						2.14, 2.04		
	γ-CH	2.64, 2.59						2.63, 2.58		
	ε-CH_3	2.15						2.13		
Glu^5	NH	8.28						8.28		
	α-CH	4.26						4.22		
	β-CH	1.94, 1.94						1.91, 1.91		
	γ-CH	2.39, 2.34						2.36, 2.31		
His^6	NH	8.43						8.42		
	α-CH	4.64						4.59		
	β-CH	3.20, 3.08						3.16, 3.06		
	2H	8.59						8.57		
	4H	7.15						7.10		
Phe^7	NH	8.23						8.19		
	α-CH	4.57						4.56		
	β-CH	2.94, 2.94						2.95, 2.95		
	2,6H	7.19						7.16		
	3,5H	7.31						7.29		
	4H	7.31						7.29		
Arg^8	NH	8.15						8.20		
	α-CH	4.28						4.24		
	β-CH	1.70, 1.66						1.62, 1.62		
	γ-CH	1.45, 1.45						1.39, 1.39		
	δ-CH	3.14, 3.14						3.10, 3.10		
	ε-NH	7.16						7.12		
	=NH	6.70						6.71		
Trp^9	NH	8.06						8.09		
	α-CH	4.78						4.73		
	β-CH	3.43, 3.28						3.42, 3.26		
	1-NH	10.18						10.18		
	2H	7.34						7.32		
	4H	7.73						7.69		
	5H	7.27						7.26		
	6H	7.23						7.20		
	7H	7.48						7.49		
Gly^{10}	NH	8.06						8.30		
	α-CH	3.91, 3.84						3.95, 3.95		
Lys^{11}	NH							8.15		
	α-CH			4.38				4.60		
	β-CH			1.95, 1.95				1.85, 1.85		
	γ-CH			1.53, 1.53				1.49, 1.49		
	δ-CH			1.75, 1.75				1.74, 1.74		
	ε-CH			3.04, 3.04				3.04, 3.04		
	ζ-NH_3^+							7.60		
Pro^{12}	α-CH			4.57				4.49		
	β-CH			2.35, 1.92				2.30, 1.92		
	γ-CH			2.06, 2.06				2.08, 2.08		
	δ-CH			3.78, 3.61				3.89, 3.66		

TABLE 1a Continued

Residue		ACTH(1–10)	ACTH(11–24)				ACTH(1–24)			
			Pro^{24}	(*trans*)	Pro^{24}	(*cis*)	Pro^{24}	(*trans*)	Pro^{24}	(*cis*)
Val^{13}	NH			8.45				8.37		
	α-CH			4.14				4.17		
	β-CH			2.11				2.12		
	γ-CH_3			1.01, 1.00				1.02, 1.02		
Gly^{14}	NH			8.48				8.51		
	α-CH			4.05, 3.89				4.06, 3.94		
Lys^{15}	NH			8.31				8.35		
	α-CH			4.33				4.36		
	β-CH			1.82, 1.82				1.87, 1.87		
	γ-CH			1.44, 1.44				1.48, 1.48		
	δ-CH			1.74, 1.74				1.75, 1.75		
	ε-CH			3.01, 3.01				3.05, 3.05		
	ζ-NH_3^+			7.57				7.60		
Lys^{16}	NH			8.42				8.43		
	α-CH			4.31				4.34		
	β-CH			1.80, 1.80				1.82, 1.82		
	γ-CH			1.45, 1.45				1.48, 1.48		
	δ-CH			1.72, 1.72				1.75, 1.75		
	ε-CH			3.01, 3.01				3.05, 3.05		
	ζ-NH_3^+			7.57				7.60		
Arg^{17}	NH			8.48				8.49		
	α-CH			4.34				4.36		
	β-CH			1.82, 1.75				1.83, 1.83		
	γ-CH			1.63, 1.63				1.67, 1.67		
	δ-CH			3.21, 3.21				3.24, 3.24		
	ε-NH			7.20				7.24		
	=NH			6.69				6.71		
Arg^{18}	NH			8.50				8.52		
	α-CH			4.63				4.66		
	β-CH			1.86, 1.77				1.90, 1.90		
	γ-CH			1.72, 1.72				1.76, 1.76		
	δ-CH			3.24, 3.24				3.26, 3.26		
	ε-NH			7.22				7.25		
	=NH			6.69				6.71		
Pro^{19}	α-CH			4.48				4.51		
	β-CH			2.31, 1.91				2.34, 1.94		
	γ-CH			2.05, 2.05				2.08, 2.08		
	δ-CH			3.85, 3.65				3.89, 3.68		
Val^{20}	NH		8.24		8.22		8.28		8.27	
	α-CH		4.09		4.10		4.13		4.15	
	β-CH		2.05		2.07		2.09		2.11	
	γ-CH_3		0.95, 0.94		0.97, 0.96		0.98, 0.98		1.00, 1.00	
Lys^{21}	NH		8.27		8.31		8.32		8.36	
	α-CH		4.31		4.35		4.33		4.38	
	β-CH		1.67, 1.67		1.77, 1.77		1.69, 1.69		1.79, 1.79	
	γ-CH		1.25, 1.25		1.34, 1.34		1.32, 1.24		1.35, 1.35	
	δ-CH		1.67, 1.67		1.68, 1.68		1.69, 1.69		1.69, 1.69	
	ε-CH		2.92, 2.92		2.95, 2.95		2.94, 2.94		2.98, 2.98	
	ζ-NH_3^+		7.54		7.54		7.57		7.57	
Val^{22}	NH		8.12		8.22		8.18		8.26	
	α-CH		4.05		4.14		4.10		4.18	
	β-CH		1.93		2.02		1.97		2.05	
	γ-CH_3		0.87, 0.80		0.93, 0.91		0.91, 0.85		0.96, 0.94	
Tyr^{23}	NH		8.31		8.14		8.40		8.19	
	α-CH		4.86		4.64		4.88		4.67	
	β-CH		3.15, 2.82		2.89, 2.89		3.17, 2.87		2.92, 2.92	
	2,6H		7.21		7.16		7.25		7.19	
	3,5H		6.84		6.86		6.87		6.89	
Pro^{24}	α-CH		4.30		3.75		4.35		3.81	
	β-CH		2.28, 1.97		1.74, 1.74		2.32, 2.02		1.78, 1.78	
	γ-CH		2.03, 2.03		1.90, 1.90		2.06, 2.06		1.97, 1.91	
	δ-CH		3.80, 3.71		3.52, 3.35		3.84, 3.72		3.56, 3.39	

TABLE 1b ^{1}H chemical shift assignment (in ppm) for ACTH(1–10), ACTH(11–24), and ACTH(1–24) in 90 mM DPC at 298 K

Residue		ACTH(1–10)	ACTH(11–24)				ACTH(1–24)			
			Pro^{24}	(*trans*)	Pro^{24}	(*cis*)	Pro^{24}	(*trans*)	Pro^{24}	(*cis*)
Ser^{1}	NH									
	α-CH	4.20						4.18		
	β-CH	4.02, 4.02						4.00, 4.00		
Tyr^{2}	NH	9.03						9.02		
	α-CH	4.69						4.66		
	β-CH	3.11, 2.99						3.10, 2.98		
	2,6H	7.18						7.16		
	3,5H	6.86						6.83		
Ser^{3}	NH	8.48						8.47		
	α-CH	4.58						4.55		
	β-CH	3.98, 3.84						3.98, 3.81		
Met^{4}	NH	8.77						8.83		
	α-CH	4.55						4.55		
	β-CH	2.24, 2.15						2.23, 2.14		
	γ-CH	2.72, 2.63						2.73, 2.61		
	ε-CH_3	2.11						2.13		
Glu^{5}	NH	8.33						8.32		
	α-CH	4.16						4.12		
	β-CH	1.96, 1.96						1.92, 1.92		
	γ-CH	2.31, 2.31						2.24, 2.24		
His^{6}	NH	8.23						8.20		
	α-CH	4.66						4.58		
	β-CH	3.25, 3.06						3.01, 3.01		
	2H	8.65						8.62		
	4H	7.17						7.10		
Phe^{7}	NH	8.11						8.00		
	α-CH	4.59						4.57		
	β-CH	3.10, 3.06						3.12, 3.02		
	2,6H	7.18						7.18		
	3,5H	7.29						7.28		
	4H	7.29						7.28		
Arg^{8}	NH	7.88						7.86		
	α-CH	4.40						4.34		
	β-CH	1.79, 1.69						1.77, 1.67		
	γ-CH	1.48, 1.48						1.45, 1.45		
	δ-CH	3.16, 3.16						3.15, 3.15		
	ε-NH	7.38						7.39		
	=NH	6.86						6.85		
Trp^{9}	NH	8.09						7.92		
	α-CH	4.75						4.68		
	β-CH	3.42, 3.21						3.40, 3.20		
	1-NH	10.62						10.60		
	2H	7.35						7.32		
	4H	7.64						7.61		
	5H	7.13						7.12		
	6H	7.09						7.07		
	7H	7.48						7.47		
Gly^{10}	NH	8.09						8.38		
	α-CH	3.89, 3.81						3.99, 3.92		
Lys^{11}	NH							8.19		
	α-CH			4.38				4.58		
	β-CH			1.96, 1.96				1.86, 1.86		
	γ-CH			1.53, 1.53				1.51, 1.51		
	δ-CH			1.75, 1.75				1.75, 1.75		
	ε-CH			3.05, 3.05				3.20, 3.20		
	ζ-NH_3^+							7.66		
Pro^{12}	α-CH			4.58				4.53		
	β-CH			2.36, 1.92				2.32, 1.94		
	γ-CH			2.06, 2.06				2.06, 2.06		
	δ-CH			3.79, 3.62				3.88, 3.66		
Val^{13}	NH			8.45				8.38		
	α-CH			4.14				4.17		
	β-CH			2.11				2.14		
	γ-CH_3			1.02, 1.01				1.02, 1.01		

TABLE 1b Continued

Residue		ACTH(1–10)	ACTH(11–24)				ACTH(1–24)			
			Pro^{24}	(*trans*)	Pro^{24}	(*cis*)	Pro^{24}	(*trans*)	Pro^{24}	(*cis*)
	γ-CH_3			1.02, 1.01					1.02, 1.01	
Gly^{14}	NH			8.48					8.55	
	α-CH			4.04, 3.90					4.01, 3.97	
Lys^{15}	NH			8.31					8.32	
	α-CH			4.34					4.35	
	β-CH			1.84, 1.84					1.87, 1.87	
	γ-CH			1.45, 1.45					1.47, 1.47	
	δ-CH			1.74, 1.74					1.75, 1.75	
	ε-CH			3.02, 3.02					3.03, 3.03	
	ζ-NH_3^+			7.59					7.66	
Lys^{16}	NH			8.42					8.38	
	α-CH			4.32					4.34	
	β-CH			1.80, 1.80					1.81, 1.81	
	γ-CH			1.46, 1.46					1.48, 1.48	
	δ-CH			1.72, 1.72					1.75, 1.75	
	ε-CH			3.02, 3.02					3.03, 3.03	
	ζ-NH_3^+			7.59					7.66	
Arg^{17}	NH			8.48					8.46	
	α-CH			4.34					4.37	
	β-CH			1.82, 1.77					1.86, 1.79	
	γ-CH			1.63, 1.63					1.66, 1.66	
	δ-CH			3.22, 3.22					3.23, 3.23	
	ε-NH			7.25					7.34	
	=NH			6.74					6.85	
Arg^{18}	NH			8.49					8.49	
	α-CH			4.63					4.64	
	β-CH			1.87, 1.77					1.89, 1.89	
	γ-CH			1.72, 1.72					1.78, 1.73	
	δ-CH			3.24, 3.24					3.25, 3.25	
	ε-NH			7.27					7.36	
	=NH			6.74					6.85	
Pro^{19}	α-CH			4.49					4.52	
	β-CH			2.31, 1.92					2.33, 1.93	
	γ-CH			2.05, 2.05					2.06, 2.06	
	δ-CH			3.86, 3.66					3.87, 3.66	
Val^{20}	NH		8.24		8.23		8.27		8.27	
	α-CH		4.09		4.10		4.14		4.14	
	β-CH		2.06		2.07		2.10		2.10	
	γ-CH_3		0.95, 0.94		0.98, 0.97		0.98, 0.98		0.98, 0.98	
Lys^{21}	NH		8.29		8.32		8.34		8.35	
	α-CH		4.32		4.37		4.36		4.38	
	β-CH		1.69, 1.69		1.76, 1.76		1.76, 1.76		1.79, 1.79	
	γ-CH		1.28, 1.28		1.34, 1.34		1.32, 1.32		1.36, 1.36	
	δ-CH		1.69, 1.69		1.70, 1.70		1.69, 1.69		1.70, 1.70	
	ε-CH		2.92, 2.92		2.95, 2.95		2.96, 2.96		2.97, 2.97	
	ζ-NH_3^+		7.56		7.56		7.62		7.62	
Val^{22}	NH		8.13		8.23		8.15		8.27	
	α-CH		4.05		4.14		4.09		4.16	
	β-CH		1.95		2.03		2.00		2.06	
	γ-CH_3		0.87, 0.80		0.93, 0.92		0.90, 0.83		0.95, 0.94	
Tyr^{23}	NH		8.22		8.07		8.20		8.05	
	α-CH		4.85		4.63		4.86		4.64	
	β-CH		3.15, 2.83		2.88, 2.88		3.16, 2.85		2.92, 2.87	
	2,6H		7.21		7.15		7.22		7.16	
	3,5H		6.84		6.86		6.85		6.88	
Pro^{24}	α-CH		4.27		3.73		4.30		3.73	
	β-CH		2.27, 1.95		1.74, 1.74		2.29, 1.97		1.76, 1.76	
	γ-CH		2.01, 2.01		1.90, 1.90		2.02, 2.02		1.93, 1.88	
	δ-CH		3.80, 3.70		3.52, 3.35		3.81, 3.68		3.54, 3.38	

TABLE 1c ^{1}H chemical shift assignment (in ppm) for ACTH(1–10), ACTH(11–24), and ACTH(1–24) in 42 mM SDS at 298 K

Residue		ACTH(1–10)	ACTH(11–24)				ACTH(1–24)			
			Pro^{24}	(*trans*)	Pro^{24}	(*cis*)	Pro^{24}	(*trans*)	Pro^{24}	(*cis*)
Ser^1	NH									
	α-CH	4.26							4.26	
	β-CH	4.08, 4.08							4.07, 4.07	
Tyr^2	NH	8.59							8.60	
	α-CH	4.74							4.73	
	β-CH	3.16, 3.00							3.15, 3.00	
	2,6H	7.23							7.23	
	3,5H	6.89							6.88	
Ser^3	NH	8.22							8.21	
	α-CH	4.58							4.57	
	β-CH	3.95, 3.88							3.95, 3.87	
Met^4	NH	8.32							8.35	
	α-CH	4.59							4.58	
	β-CH	2.28, 2.18							2.29, 2.19	
	γ-CH	2.72, 2.64							2.72, 2.62	
	ε-CH_3	2.14							2.11	
Glu^5	NH	8.15							8.20	
	α-CH	4.25							4.22	
	β-CH	1.99, 1.95							1.95, 1.95	
	γ-CH	2.37, 2.37							2.30, 2.30	
His^6	NH	8.18							8.23	
	α-CH	4.63							4.66	
	β-CH	3.07, 3.07							3.21, 3.13	
	2H	8.66							8.66	
	4H	7.20							7.27	
Phe^7	NH	7.95							7.92	
	α-CH	4.65							4.64	
	β-CH	3.14, 3.04							3.15, 3.09	
	2,6H	7.29							7.29	
	3,5H	7.41							7.41	
	4H	7.41							7.41	
Arg^8	NH	7.71							7.65	
	α-CH	4.23							4.26	
	β-CH	1.64, 1.59							1.59, 1.59	
	γ-CH	1.09, 1.09							1.17, 1.17	
	δ-CH	3.03, 3.03							3.06, 3.06	
	ε-NH	6.97							7.00	
	=NH	6.69								
Trp^9	NH	7.32							7.30	
	α-CH	4.81							4.74	
	β-CH	3.46, 3.26							3.44, 3.21	
	1-NH	9.93							9.96	
	2H	7.34							7.34	
	4H	7.61							7.45	
	5H	7.11							7.13	
	6H	7.11							7.09	
	7H	7.40							7.41	
Gly^{10}	NH	7.93							7.97	
	α-CH	3.97, 3.97							4.10, 3.91	
Lys^{11}	NH								7.76	
	α-CH			4.39					4.58	
	β-CH			2.02, 2.02					1.88, 1.88	
	γ-CH			1.59, 1.59					1.51, 1.51	
	δ-CH			1.80, 1.80					1.78, 1.78	
	ε-CH			3.10, 3.10						
	ζ-NH_3^+									
Pro^{12}	α-CH			4.64					4.61	
	β-CH			2.41, 1.98					2.36, 2.03	
	γ-CH			2.06, 2.06					2.09, 2.09	
	δ-CH			3.85, 3.62					3.86, 3.68	

TABLE 1c Continued

Residue		ACTH(1–10)	ACTH(11–24)				ACTH(1–24)			
			Pro^{24}	(*trans*)	Pro^{24}	(*cis*)	Pro^{24}	(*trans*)	Pro^{24}	(*cis*)
Val^{13}	NH			7.96					8.08	
	α-CH			4.24					4.22	
	β-CH			2.18					2.24	
	γ-CH_3			1.01, 1.01					1.06, 1.06	
Gly^{14}	NH			8.29					8.35	
	α-CH			4.03, 4.03					4.06, 4.06	
Lys^{15}	NH			8.08					8.06	
	α-CH			4.34					4.39	
	β-CH			1.92, 1.92					1.94, 1.94	
	γ-CH			1.49, 1.49					1.48, 1.48	
	δ-CH			1.82, 1.82					1.85, 1.85	
	ε-CH			3.03, 3.03					3.09, 3.09	
	ζ-NH_3^+									
Lys^{16}	NH			8.26					8.24	
	α-CH			4.29					4.36	
	β-CH			1.87, 1.87					1.90, 1.90	
	γ-CH			1.47, 1.47					1.51, 1.51	
	δ-CH			1.74, 1.74					1.78, 1.78	
	ε-CH			3.05, 3.05					3.07, 3.07	
	ζ-NH_3^+									
Arg^{17}	NH			8.06					8.09	
	α-CH			4.36					4.42	
	β-CH			1.92, 1.80					1.85, 1.85	
	γ-CH			1.68, 1.68					1.71, 1.71	
	δ-CH			3.23, 3.23					3.28, 3.28	
	ε-NH			7.24					7.28	
	=NH									
Arg^{18}	NH			7.97					8.02	
	α-CH			4.60					4.65	
	β-CH			1.92, 1.81					1.97, 1.87	
	γ-CH			1.71, 1.71					1.76, 1.76	
	δ-CH			3.25, 3.25					3.29, 3.29	
	ε-NH			7.21					7.26	
	=NH									
Pro^{19}	α-CH			4.54					4.58	
	β-CH			2.35, 2.10					2.38, 2.02	
	γ-CH			2.00, 2.00					2.11, 2.11	
	δ-CH			3.80, 3.73					3.85, 3.78	
Val^{20}	NH		8.00		8.04		8.03		8.08	
	α-CH		4.10		4.15		4.16		4.21	
	β-CH		2.13		2.10		2.17			
	γ-CH_3		0.98, 0.98		1.01, 1.01		1.01, 1.01			
Lys^{21}	NH		8.14		8.20		8.18		8.23	
	α-CH		4.31		4.38		4.36		4.43	
	β-CH		1.72, 1.72				1.90, 1.90			
	γ-CH		1.44, 1.33				1.40, 1.40			
	δ-CH		1.72, 1.72				1.77, 1.77			
	ε-CH		3.01, 3.01				3.05, 3.05			
	ζ-NH_3^+									
Val^{22}	NH		7.84		8.00		7.87		8.08	
	α-CH		4.06		4.12		4.12		4.18	
	β-CH		2.00		2.10		2.05		2.14	
	γ-CH_3		0.90, 0.82		0.94, 0.94		0.94, 0.87		0.98, 0.98	
Tyr^{23}	NH		8.12		7.86		8.15		7.92	
	α-CH		4.85		4.65		4.89		4.69	
	β-CH		3.14, 2.84		2.90, 2.83		3.17, 2.89		2.95, 2.88	
	2,6H		7.21		7.14		7.24		7.18	
	3,5H		6.84		6.87		6.88		6.91	
Pro^{24}	α-CH		4.29		3.65		4.34		3.71	
	β-CH		2.27, 1.99		1.91, 1.83		2.31, 2.02		1.96, 1.88	
	γ-CH		2.02, 2.02		1.74, 1.74		2.05, 2.05		1.78, 1.78	
	δ-CH		3.77, 3.63		3.52, 3.37		3.82, 3.65		3.56, 3.41	

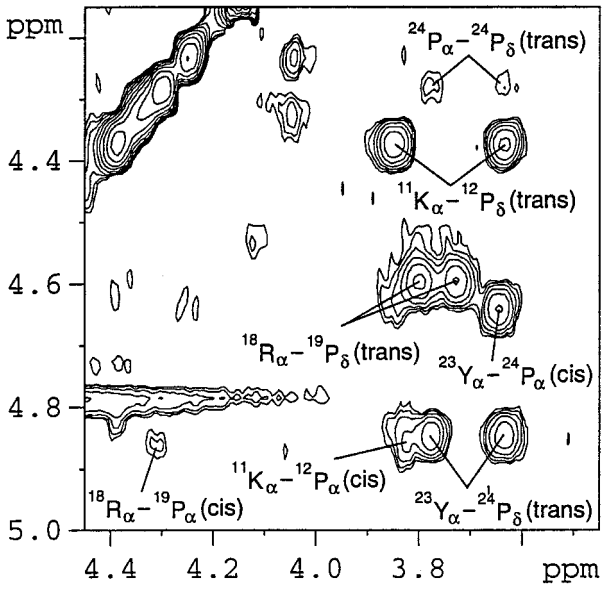

FIGURE 2 The X-Pro αH-αH and αH-δH region in the NOESY map of ACTH (11–24) in 42 mM SDS micelles at 298 K. For Pro^{24}, both the α-α (*cis*) and α-δ (*trans*) correlations were clearly observed for Tyr^{23}-Pro^{24}, indicating the existence of both *trans* and *cis* Tyr^{23}-Pro^{24} isomers. For Pro^{12} and Pro^{19}, weaker α-α correlations were also present, in addition to the strong α-δ correlations. α-α correlations for Pro^{12} and Pro^{19} are too weak to be detected in DPC micelles and in water.

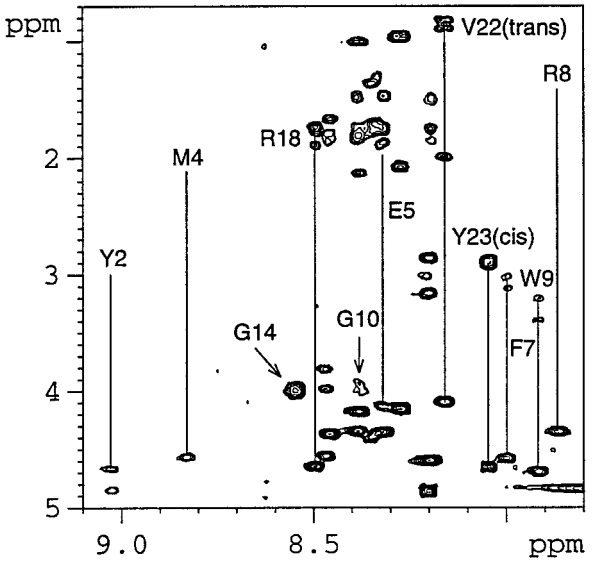

FIGURE 3 The NH-αH region of the TOCSY map of ACTH (1–24) in 98 mM DPC micelles at 298 K. Because of the shorter T_2 of the NH protons of the residues 1–10, the TOCSY correlations for residues 1–10 are noticeably weaker than those of residues 11–24. Some long-range (e.g., NH-βH and NH-γH) correlations for the former did not appear.

the difference in the order parameter of the residues. For the residues 11–24, the reduced restriction of their motion would result in much lower order parameters and thus a longer T_2.

NH chemical shifts

The NH chemical shifts, δ(NH), are the most revealing of the environment of the peptides, and in the present work, the δ(NH) provide a clear description of the binding picture for the ACTH peptides in these two micelles. The salient features of the δ(NH) results are given as follows.

1. In both SDS and DPC micelles, the δ(NH) of ACTH (1–10) and ACTH (11–24) are practically identical to the corresponding segments in ACTH (1–24) (to well within 0.1 ppm, with only three exceptions, where the differences were 0.17, 0.12, and 0.11 ppm, respectively), implying that all of the corresponding segments of these peptides in a given micelle are in similar physical environments (Figs. 4 and 5).

2. For SDS micelles, the δ(NH) of many residues in both the 1–10 and the 11–24 segments are significantly shifted upfield (by as much as 0.7 ppm) from those in water (Fig. 4). This supports the conclusion from diffusion measurements that all of these segments have high partition coefficients in SDS micelles. The large upfield shift may imply that these peptides are inserted into the hydrophobic interior of the SDS micelles, although formation of a helical secondary structure (see next section) may also contribute to the upfield shift of δ(NH).

3. For DPC micelles, δ(NH) in the 1–10 segments deviate from those in water. There are both upfield and downfield shifts. However, for the 11–24 segments, δ(NH) are practically identical to the corresponding values in water (Fig. 5).

In the aqueous samples of these three peptides, the linewidths are sufficiently narrow to enable the $^3J_{NH\text{-}\alpha H}$ to be determined, and all of their values fell between 6 and 8 Hz, except for Gly^{10}, the average $^3J_{NH\text{-}\alpha H}$ of which is 5.5 Hz. This range of values is characteristic of those expected for random structures (Wuthrich, 1986). Because of increases in the linewidths in SDS samples, no determination of the J couplings is possible. For the 1–10 segment in DPC micelles, the $^3J_{NH\text{-}\alpha H}$ for residues Tyr^2-His^6 and Arg^8 was <6 Hz (Table 2). The NH resonances of Phe^7 and Trp^9 overlapped with each other, preventing the determination of the J coupling for these residues. Among those $^3J_{NH\text{-}\alpha H}$ of residues 11–24 measured, the value was between 6 and 8 Hz.

Secondary structure

From the paucity of nonsequential NOE for the ACTH peptides in water, and the complete lack of N_i-N_{i+1} correlations from both the NOESY and ROESY spectra, it can be concluded that all three peptides are in the random coil conformation in water. This contradicts the results of a previous study (Toma et al., 1981), which asserted that the N-terminus of ACTH (1–24) exhibits "α-helix type organization" in water, based on ^{13}C chemical shifts.

In the two previous studies of ACTH (1–10), Rawson et al. (1982) concluded that ACTH (1–10) is in random coil

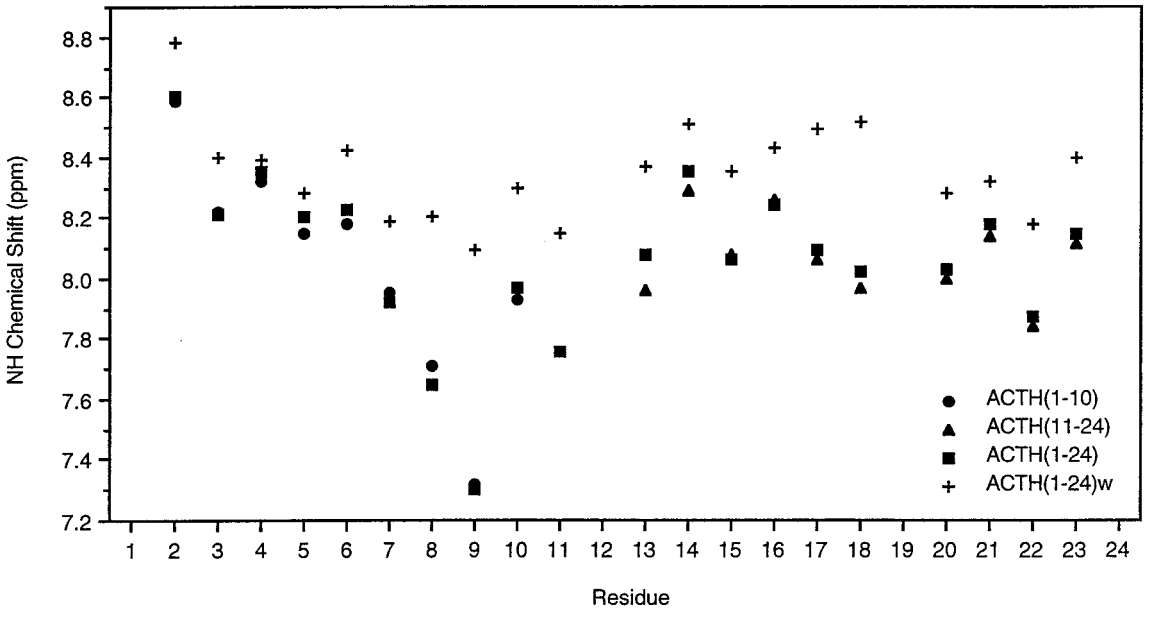

FIGURE 4 The NH chemical shifts, δ(NH), of ACTH (1–24) (■), ACTH (1–10) (●), and ACTH (11–24) (▲), in 42 mM SDS micelles, and ACTH (1–24) in water (+) at 298 K. For the 1–24 and 11–24 fragments, the δ(NH) for the major isomeric form (the *trans*-Pro^{24} isomer) were presented. Note that δ(NH) of all corresponding residues are practically identical for these three ACTH fragments in SDS micelles.

conformation in water, and does not have a dominant contribution from helical conformations, even in trifluoroethanol. Tunga et al. concluded that ACTH (1–10) prefers extended, albeit different conformations in both water and dimethylsulfoxide. In a circular dichroism (CD) study (Greef et al., 1976), it was reported that all ACTH peptides have random coil conformation in water. ACTH (1–39) and its N-terminal fragments exhibit α-helical conformation in trifluoroethanol, whereas its C-terminal fragments are random, even in organic solvents.

In DPC micelles, both ACTH (1–10) and the 1–10 segment of ACTH (1–24) exhibit characteristics of a folded

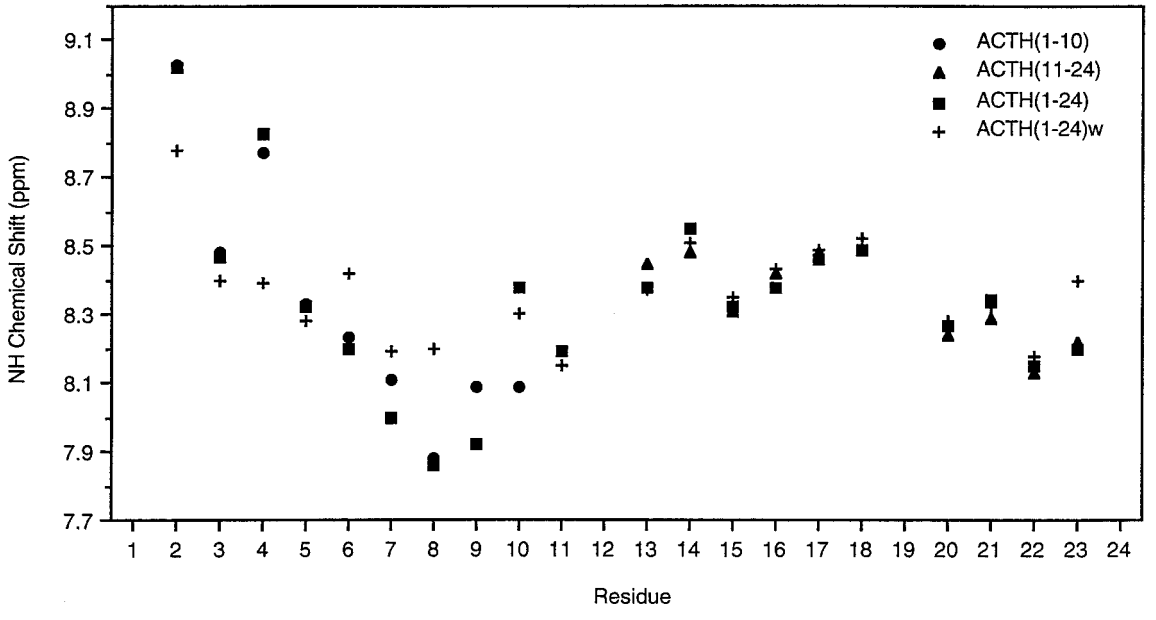

FIGURE 5 The NH chemical shifts, δ(NH), of ACTH (1–24) (■), ACTH (1–10) (●), and ACTH (11–24) (▲) in 98 mM DPC micelles, and ACTH (1–24) in water (+) at 298 K. For the 1–24 and 11–24 fragments, the δ(NH) for the major isomeric form (the *trans*-Pro^{24} isomer) were presented. Note that δ(NH) of all corresponding residues are practically identical for these three ACTH fragments in DPC micelles. The large apparent difference in Gly^{10} is due to the fact that Gly^{10} is the terminal residue in ACTH (1–10), but an interior residue in ACTH (1–24). Note also that the δ(NH) for the 11–24 residues are practically identical to the corresponding values in water.

TABLE 2 NOE* and $^3J_\alpha N$ (in Hz) of ACTH peptides in 98 mM DPC micelles at 298K

	ACTH (1–10)										ACTH (11–24)#													
	S1	Y2	S3	M4	E5	H6	F7	R8	W9	G10	K11	P12	V13	G14	K15	K16	R17	R18	P19	V20	K21	V22	Y23	P24
$^3J(\alpha N)$		<6	<6	<6	<6	<6		<6		<6			8.0			6.6						8.1		
$\alpha N(i,i+1)$	s	s	s	s	s	s	s	s	s			m	m	m	s	s	s		s	s	s	m		
$NN(i,i+1)$		m	s	s	m	m	s	s	a												w	w		
$\alpha N(i,i+2)$	w	w	a	m	m		w	w							a	a								
$NN(i,i+2)$			w	w	w	w	a	a																
$\alpha N(i,i+3)$		a	a	a	w										a		a							
$\alpha\beta(i,i+3)$		a	a	a											a			a						
$\alpha N(i,i+4)$			a														a		a					
$NN(i,i+3)$			w	w																				
$\beta N(i,i+3)$			w	w		a									a					a				

	ACTH (1–24)#																							
	S1	Y2	S3	M4	E5	H6	F7	R8	W9	G10	K11	P12	V13	G14	K15	K16	R17	R18	P19	V20	K21	V22	Y23	P24
$^3J(\alpha N)$																						8.3		
$\alpha N(i,i+1)$	s	s	s	s	s	s	s	s	s	s		s	s	s	s	s	s		s	s	s	s		
$NN(i,i+1)$		m	m	s	m	s	s	m	s	m			m	m							w			
$\alpha N(i,i+2)$	w		a	a	m	a	m	a	w			w	a	a		a			a		a			
$NN(i,i+2)$					w						a			a							a			
$\alpha N(i,i+3)$			a	a	w	a	a	w		a		a	a							a				
$\alpha\beta(i,i+3)$		a	a	a				a		a					a			a		a				
$\alpha N(i,i+4)$			a	a			a		a		a	a					a							
$NN(i,i+3)$																								
$\beta N(i,i+3)$			a	a		a	a	a					a		a				a					

*The strength of NOEs are classified as strong (s), medium (m) and weak (w). The other NOEs are ambiguous (a) due to overlapping of signals.
#NOE data for the trans-Pro^{24} isomer only.

structure (Table 2). For ACTH (1–24) there is a clear difference in the conformational characteristics between those of the 1–10 segment and those of the 11–24 segment. As shown in Fig. 6, the NH-NH region of the NOESY map revealed continuous and strong correlations of the N_i-N_{i+1} type in the 1–10 segment. There are also a few weaker N_i-N_{i+2} correlations, such as 5–7, 6–8, 7–9, and 8–10. In contrast, in the 11–24 segment, only three weak N_i-N_{i+1} correlations, ^{13}V-^{14}G, ^{14}G-^{15}K, and ^{21}K-^{22}V, are evident. In addition, a ^{22}V-^{23}W correlation of the minor *cis*-Pro$_{24}$ isomer was also present.

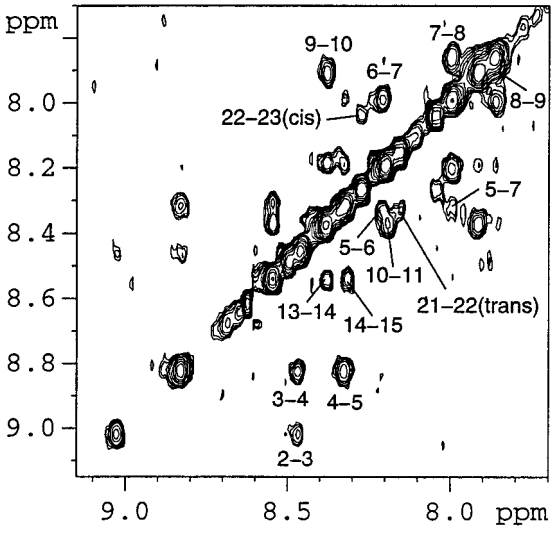

FIGURE 6 The NH-NH region of the NOESY map of ACTH (1–24) in 98 mM DPC micelles at 298 K. Note that strong N_i-N_{i+1} correlations persist throughout the 1–10 segment. Even some N_i-N_{i+2} are observed (not all are labeled). For the 11–24 segment, only a few weaker N_i-N_{i+1} correlations exist.

Many α_i-N_{i+2} and some α_i-N_{i+3} correlations were observed for the residues in the 1–10 segment. The prominence of the α_i-N_{i+2} cross-peaks in the 1–10 segment may indicate the likelihood of a 3_{10} helix. However, some α_i-N_{i+3} cross-peaks expected of any helical structures were missing from the NOESY of the 1–10 segments. Therefore, the preference for a helical structure in this segment cannot be firmly established. The 11–24 segment of ACTH (1–24) and ACTH (11–24) exhibits little secondary structure, as in water, as indicated by the discontinuity in and the weakness of the N_i-N_{i+1} correlations in ACTH (1–24) and the lack of N_i-N_{i+1} correlations in ACTH (11–24). For the 11–24 segment, all of the α_i-N_{i+2} and α_i-N_{i+3} correlations fell into the "ambiguous" category because of overlap, and thus cannot be confirmed. The secondary structure of ACTH (1–24) in DPC micelles is in essential agreement with the results of Schwyzer et al. (Gysin and Schwyzer, 1984; Gremlich et al., 1983, 1984) for ACTH (1–24) in POPC bilayers.

In SDS micelles, all three peptides exhibit distinct characteristics of an induced secondary structure (N_i-N_{i+1} correlations throughout the chain, and other nonsequential α-N and α-β NOE correlations). Unlike these peptides in DPC

micelles, there are no distinct differences in the NOE patterns between the 1–10 and the 11–24 segments (Table 2). The NOE pattern for the 1–10 segment is quite similar to that in the DPC micelles. There is probably a 3_{10} helix formation in the 1–10 segment in both ACTH (1–10) and in ACTH (1–24), but this conclusion is not certain, because some α_i-N_{i+3} cross-peaks expected of a helical structure were also missing, as in the DPC case. The folding in the 11–24 segment does not follow a simple pattern. Severe overlap of signals hampers more unambiguous assignment of the long-range NOEs, causing difficulties in identifying the secondary structure. The overlap was due to the large number of repeating residues (there are three Pro, three Val, four Lys, and two Arg in the 11–24 segment) and to the existence of *trans-cis* isomerism at all three proline sites discussed above.

DISCUSSION

The present results on the partition of the ACTH peptides in the SDS and DPC micelles showed that the partition patterns for the ACTH peptides in these two micelles are different. The partition coefficients for all three peptides in the SDS micelles are $>10^3$ (Table 1). Results obtained in this laboratory for another series of peptides characterized by primary amphiphilicity—substance P (+3 charge at neutral pH), neurokinin A (+1 charge), and even the negatively charged (−1 charge) neurokinin B—showed that all the partition coefficients are greater than 10^3 in 42 mM SDS micelles (Wong, unpublished observations). The propensity of SDS to partition peptides ranging from hydrophobic to highly charged is clearly demonstrated in our studies. Both the electrostatic and the hydrophobic interactions are effective in causing partitioning of the peptides in SDS micelles. For the zwitterionic DPC micelles, however, only the hydrophobic interaction appears to be effective in causing partitioning of the peptides, as evidenced by the low partitioning of the charged ACTH (11–24), with a partition coefficient of only 7.3 ± 0.1 (Table 1), orders of magnitude lower than that of the other peptides.

Schwyzer et al., in a series of papers (Gysin and Schwyzer, 1984; Gremlich et al., 1983, 1984), determined the binding of ACTH (1–10), ACTH (1–24), and ACTH (11–24) to lipid bilayers by using ATR-IR and hydrophobic photolabeling. The main conclusions from their work (Schwyzer, 1992) were that ACTH (1–10) does not interact hydrophobically with neutral or anionic bilayers—it is not adsorbed into these bilayers from solution, and the trapped ACTH (1–10) in dry bilayers readily escapes into the aqueous phase upon hydration. ACTH (11–24) is also not adsorbed into neutral bilayers, but the trapped peptide is not washed out from the dry bilayers. On the other hand, ACTH (1–24) was found to be firmly incorporated into the membrane by inserting the 1–10 hydrophobic segment perpendicularly into the hydrophobic core of the bilayer, while the charged 11–24 segment remains on the aqueous membrane

TABLE 3 NOE* and $^3J_{\alpha N}$ (in Hz) of ACTH peptides in 42 mM SDS micelles at 298K

	ACTH (1–10)										ACTH (11–24)#													
	S1	Y2	S3	M4	E5	H6	F7	R8	W9	G10	K11	P12	V13	G14	K15	K16	R17	R18	P19	V20	K21	V22	Y23	P24
$^3J(\alpha N)$		5.8	<6		<6	6.6				5.8														
$\alpha N(i,i+1)$	s	s	s	s	s	s	s	s	s			s	s	s	s	s	s		s	s	s	s		
$NN(i,i+1)$		m	w	s	a	s	m	s	s				s	s	s	s	m			m	s	s		
$\alpha N(i,i+2)$	w	w	a	w	m	a	a	w			a	m	w	m	a	a			w	a	a			
$NN(i,i+2)$													a	a	a	a		a			a			
$\alpha N(i,i+3)$	a		a			a								a	a		a			a				
$\alpha\beta(i,i+3)$				a								a		a	a		a	a	a		a			
$\alpha N(i,i+4)$	a															a								
$NN(i,i+3)$														a	a		a			a				
$\beta N(i,i+3)$															a		a			a				

	ACTH (1–24)#																							
	S1	Y2	S3	M4	E5	H6	F7	R8	W9	G10	K11	P12	V13	G14	K15	K16	R17	R18	P19	V20	K21	V22	Y23	P24
$^3J(\alpha N)$																								
$\alpha N(i,i+1)$	s	s	s	s	s	s	s	s	s	s		s	s	s	s	s	s		s	s	s	s		
$NN(i,i+1)$		m	m	s	a	s	m	w	w	s			s	s	s	s	m			m	s	s		
$\alpha N(i,i+2)$		w	a	a	m	a	a	w	w		a		a	w	a	a		a	a	a	a			
$NN(i,i+2)$			a	a	a	a							a		a	a		a			a			
$\alpha N(i,i+3)$		a	a			a					a	a	a	a	a		a	a		a				
$\alpha\beta(i,i+3)$	a			w		a								w	a			a	a					
$\alpha N(i,i+4)$		a									a		a	a		a								
$NN(i,i+3)$			a				a						a	a	a		a							
$\beta N(i,i+3)$	a	a	a	a		a	a					a			a		a	a						

*The strength of NOEs are classified as strong (s), medium (m) and weak (w). The other NOEs are ambiguous (a) due to overlapping of signals.
#NOE data for the trans-Pro^{24} isomer only.

surface. Furthermore, the inserted segment was found to adopt a helical structure. The above observations led Schwyzer to propose that both the hydrophobic 1–10 and the charged 11–24 segments are needed for membrane binding. These findings for ACTH constituted a main part of the data central to supporting Schwyzer's message-address (Schwyzer, 1977; Sargent and Schwyzer, 1986) and membrane compartments (Schwyzer, 1986, 1991) concepts. The "compartments" were defined as the hydrophobic core, the water/headgroup interface, and the aqueous phase of the membrane system. According to these concepts, the address segments of the peptides "direct" the peptides to different membrane compartments, and resulting in the peptides binding to different receptors, as in the case of ACTH (1–10) and ACTH (1–24), which bind to central nervous system and steroidogenic receptors, respectively. Our preliminary diffusion results on the ACTH/POPC vesicle system are also in essential agreement with the above binding results, albeit not necessarily with the interpretation of Schwyzer.

There are major differences between the results of Schwyzer et al. and our diffusion results on the ACTH/vesicle systems on the one hand and the micellar results of this work on the other (Table 1). We have found in this work that ACTH (1–10) is almost completely partitioned in both SDS and DPC micelles, contrary to the bilayer results of Schwyzer, which showed that ACTH (1–10) does not partition into neutral or anionic bilayers. In addition, it is found in the present work that the highly charged (at neutral pH) ACTH (11–24) does not partition significantly into the DPC micelles, although its partition in negatively charged SDS micelles is practically complete. This is also contradictory to Schwyzer's finding on the relative affinities of ACTH (1–10) and ACTH (11–24) to neutral bilayers. From the consideration of the electrostatic and hydrophobic contribution to the partitioning, the present results for ACTH (11–24) are quite expected. Because only the hydrophobic interactions are responsible for partitioning of the ACTH peptides into DPC micelles, the highly charged ACTH (11–24) (+6 at neutral pH) should prefer to stay in the aqueous phase rather than be partitioned in the uncharged DPC micelles.

The 1–24 peptide was found in this work to be almost completely partitioned in both the SDS and the DPC micelles as well. However, even though partition or binding for the whole peptide in DPC micelles is high, the hydrophobic 1–10 segment and the hydrophilic 11–24 segment were found to interact with the micelle differently. There are drastic differences in the linewidths (as manifested in the TOCSY intensities), the δ(NH), and the NOE patterns for the two segments. These results all pointed toward one interpretation, i.e., the 1–10 segment is "bound" to the DPC micelles, whereas the 11–24 segment protrudes into the aqueous phase with no significant interaction with the micelles.

It should be noted, though, that the "partition" of the peptides as determined from diffusion measurements does not provide information on where the peptides or certain segments are located in the micelles. Because "partitioning" or "binding" as defined in the diffusion study requires only that the peptide binds to a micelle and diffuse as a peptide/micelle entity for a period of time longer than the diffusion time (~50 ms), it does not discriminate between partitioning in the interior core of the micelles and binding on the surface of the micelles.

No quantitative examination of partition of peptides in micelles has been made in the past. Keire and Fletcher (1996) suggested that there are differences in the kinetics of binding of SP with SDS and DPC micelles. Whereas SP binds "completely" with SDS micelles, its exchange between free form and DPC-bound form is fast in the pertinent NMR time scale but slow in the CD time scale. However, their study did not examine the equilibrium of partitioning.

There are no differences in the secondary structure in the 1–10 segment, either between ACTH (1–10) and ACTH (1–24), or between different micelles. It is important to note that for this active message (1–10) segment, a partial helical structure (or an alternative folded structure) is conserved in all cases. It appears that the conformation of this segment is not sensitive to the exact chemical or physical details of the hydrophobic environment. The major differences in the secondary structure of these peptides in the two micelles are manifested in the 11–24 segment, arising from the differences in the binding of this segment in these two micelles. When the 11–24 segment is in the aqueous environment, as in the DPC micellar samples and in aqueous samples, it exhibits little secondary structure. In contrast, when it is partitioned into the hydrophobic environment or bound to the surface of the micelles as in the SDS case, significant NOE correlations indicate the formation of a definite secondary structure. A molecular dynamics simulation of the interaction of ACTH (1–24) with an explicit SDS micelle (MacKerell, 1995), incorporating the NOEs obtained in this study, is under way in this laboratory to further elucidate the mode of binding of this peptide (position and orientation with respect to the headgroup/water interface, and specific interactions with the headgroup) and the conformation of the partitioned peptide.

In summary, the partition, the secondary structure, the linewidths, and the δ(NH) presented a coherent picture of the binding of the ACTH peptides in these two micelles with the following significant implications:

1. The binding patterns of the ACTH peptides with SDS and DPC micelles are different from each other, and they differ significantly from their binding to neutral POPC bilayers and vesicles. This affirms our proposal that the validity of the assumption that micelles are good membrane mimics needs to be investigated more closely. There are difference in the secondary structure as well, specifically in the 11–24 segment. The difference is a direct result of whether this particular segment is in the hydrophobic core of the micelles or bound to the micellar surface (as in the SDS micelles), or is in the aqueous environment (as in the DPC micelles). However, when a segment of the peptide is

in a hydrophobic or surface-bound environment, as in the 1–10 segment, the same secondary structure was observed in SDS and DPC micelles, and in POPC bilayers (Gysin and Schwyzer, 1984; Gremlich et al., 1984).

2. In a given micellar medium, all corresponding fragments of these peptides reside in exactly the same membrane environment. That is, the 1–10 segment, for example, interacts with a certain micelle (DPC, for example) in exactly the same way and resides in exactly the same membrane location, whether it exists by itself or as a part of the 1–24 segment. The same applies to the 11–24 segment. If these micelles really mimic membranes in interacting with the ACTH peptides, the present results contradict the membrane-mediated hormone action (Sargent and Schwyzer, 1986) and the membrane compartments (Schwyzer, 1986, 1991) concepts, that different address segments of the peptides (in this case, the presence and the absence of the 11–24 segment) direct the message segment (the 1–10 segment) to different compartments in the membrane/water system, thus causing the peptides to bind to different receptors. However, the results of this work cast doubt on whether the ACTH peptides bind to micelles in the same way as they bind to membranes (see conclusion no. 1).

The 500-MHz spectrometer was purchased in part through a grant from the National Science Foundation (CHE-89-08304). Partial financial support from the Research Council of the University of Missouri, Columbia, MO, is also gratefully acknowledged.

REFERENCES

Barenholz, Y., D. Gibbes, B. J. Litman, J. Goll, T. E. Thompson, and F. D. Carlson. 1977. A simple method for the preparation of homogeneous phospholipid vesicles. *Biochemistry.* 16:2806–2810.

Bax, A., and D. G. Davis. 1985. Practical aspects of two-dimensional transverse NOE spectroscopy. *J. Magn. Reson.* 63:207–213.

Bax, A., M. Ikura, L. E. Kay, D. A. Torchia, and R. Tschudin. 1990. Comparison of different modes of two-dimensional reverse-correlation NMR for the study of proteins. *J. Magn. Reson.* 86:304–318.

Beschiaschvili, G., and J. Seelig. 1992. Peptide binding to lipid bilayers: nonclassical hydrophobic effect and membrane-induced pK shifts. *Biochemistry.* 31:10044–10053.

Bodenhausen, G., H. Kogler, and R. R. Ernst. 1984. Selection of coherence transfer pathways in NMR pulse experiments. *J. Magn. Reson.* 58: 370–388.

Brun, T. S., H. Hoiland, and E. Vikingstad. 1978. Partial molal volume and isentropic partial molal compressibilities of surface active agents in aqueous solution. *J. Colloid Interface Sci.* 63:89–96.

Bystrov, V. F., N. I. Duborvina, L. J. Barsukov, and L. D. Bergelson. 1971. NMR differentiation of the internal and external phospholipid membrane surfaces using paramagnetic Mn^{2+} and Eu^{3+} ions. *Chem. Phys. Lipids.* 6:343–350.

Croonen, Y., E. Gelade, M. Van der Zegel, N. Van der Auweraer, H. Vandendriessche, F. C. DeSchryver, and M. Almgren. 1983. Influence of salt, detergent concentration, and temperature on the fluorescence quenching of 1-methylpyrene in sodium dodecylsulfate with *m*-dichlorobenzene. *J. Phys. Chem.* 87:1426–1431.

Davis, D. G., and A. Bax. 1985. Assignment of complex ^{1}H NMR spectra via two-dimensional homonuclear Hartman-Hahn spectroscopy. *J. Am. Chem. Soc.* 107:2820–2821.

Greef, D., F. Toma, S. Fermandjian, M. Low, and L. Kisfaludy. 1976. Conformational studies of corticotropin$_{1-32}$ and constitutive peptides by circular dichroism. *Biochim. Biophys. Acta.* 439:219–231.

Gremlich, H. U., U. P. Frigeli, and R. Schwyzer. 1983. Conformational changes of adrenocorticotropin peptides upon interaction with lipid membranes revealed by infrared attenuated total reflection spectroscopy. *Biochemistry.* 22:4257–4264.

Gremlich, H. U., U. P. Frigeli, and R. Schwyzer. 1984. Interaction of adrenocorticotropin-(11–24)-tetradecapeptide with neutral lipid membranes revealed by infrared attenuated total reflection spectroscopy. *Biochemistry.* 23:1808–1810.

Griesinger, G., G. Ottling, K. Wuthrich, and R. R. Ernst. 1988. TOCSY for ^{1}H spin system identification in macromolecules. *J. Am. Chem. Soc.* 110:7870–7872.

Gysin, B., and R. Schwyzer. 1984. Hydrophobic and electrostatic interactions between adrenocorticotropin-(1–24)-tetracosapeptide and lipid vesicles. Amphiphilic primary structures. *Biochemistry.* 23:1811–1818.

Itri, R., and L. Q. Amaral. 1991. Distance distribution function of sodium dodecylsulfate micelles by x-ray scattering. *J. Phys. Chem.* 95:423–427.

Jeener, J., B. Meier, P. Bachman, and R. R. Ernst. 1979. Investigation of exchange processes by two-dimensional NMR spectroscopy. *J. Chem. Phys.* 71:4546–4553.

Jonsson, B., H. Wennerstrom, P. G. Nilsson, and P. Linse. 1986. Self-diffusion of small molecules in colloidal systems. *Colloid Polym. Sci.* 264:77–84.

Kallick, D. A., M. R. Tessmer, C. R. Watts, and C. V. Li. 1995. The use of dodecylphosphocholine micelles in solution NMR. *J. Magn. Reson. Ser. B.* 109:60–65.

Keire, D., and T. G. Fletcher. 1996. The conformation of substance P in lipid environment. *Biophys. J.* 70:1716–1727.

Kumar, A., R. R. Ernst, and K. Wuthrich. 1980. A two-dimensional nuclear Overhauser enhancement (2D NOE) experiment for the elucidation of complete proton-proton cross relaxation networks in biological macromolecules. *Biochim. Biophys. Res. Commun.* 95:1–10.

Lauterwein, J., C. Bosch, L. R. Brown, and K. Wuthrich. 1979. Physicochemical studies of the protein-lipid interactions in melittin-containing micelles. *Biochim. Biophys. Acta.* 556:244–264.

MacKerell, A. D. 1995. Molecular dynamics simulation analysis of a sodium dodecyl sulfate micelle in aqueous solution. Decreased fluidity of the micelle hydrocarbon interior. *J. Phys. Chem.* 99:1946–1855.

Mills, R. 1973. Self-diffusion in normal and heavy water in the range 1–45°. *J. Phys. Chem.* 77:685–688.

Morris, K. F., C. S. Johnson, Jr., and T. C. Wong. 1994. Diffusion study of the polymer-induced non-Newtonian to Newtonian transition in the viscoelastic CTAB/sodium salicylate/water system by diffusion ordered spectroscopy (DOSY). *J. Phys. Chem.* 98:603–608.

Rawson, B. J., J. Feeney, and B. J. Kimber. 1982. ^{1}H nuclear magnetic resonance studies of the conformations of adrenocorticotropic hormone ACTH (1–10) and related peptides in aqueous and trifluoroethanol solutions. *J. Chem. Soc. Perkin Trans. II.* 1471–1477.

Sargent, D. F., and R. Schwyzer. 1986. Membrane lipid phase as catalyst for peptide-receptor interactions. *Proc. Natl. Acad. Sci. USA.* 83: 5774–5778.

Schwyzer, R. 1977. ACTH: a short introductory review. *Ann. N.Y. Acad. Sci.* 297:3–26.

Schwyzer, R. 1986. Molecular mechanism of opioid receptor selection. *Biochemistry.* 25:6335–6342.

Schwyzer, R. 1991. Peptide membrane interactions and a new principle in quantitative structure activity relationships. *Biopolymers.* 31:785–792.

Schwyzer, R. 1992. Conformations and orientations of amphiphilic peptides induced by artificial lipid membranes: correlations with biological activity. *Chemtracts Biochem. Mol. Biol.* 3:347–379.

Seelig, J., S. Nebel, P. Ganz, and C. Bruns. 1993. Electrostatic and nonpolar peptide-membrane interactions. Lipid binding and functional properties of somatostatin analogues of charge $z = +1$ to $z = +3$. *Biochemistry.* 32:9714–9721.

Shaka, A. J., and R. Freeman. 1983. Simplification of NMR spectra through multiple-quantum coherence. *J. Magn. Reson.* 51:169–173.

Sklenar, V., M. Piotto, R. Leppik, and V. Saudek. 1993. Gradient-tailored water suppression for ^{1}H-^{15}N HSQC experiments optimized to retain full sensitivity. *J. Magn. Reson. Ser. A.* 102:241–245.

Soderman, O., G. Carlstrom, U. Olsson, and T. C. Wong. 1988. NMR relaxation in micelles. ^{2}H relaxation at three field strengths of three positions on the alkyl chain of sodium dodecyl sulfate. *J. Chem. Soc. Faraday Trans. 1.* 84:4475–4486.

Stilbs, P. 1982. Fourier transform NMR pulsed-gradient spin-echo (FT-PGSE) self-diffusion measurements of solubilization equilibria in SDS solutions *J. Colloid Interface Sci.* 87:385–394.

Stilbs, P. 1983. A comparative study of micellar solubilization for combinations of surfactants and solubilizates using the Fourier transform pulsed-gradient spin-echo NMR multicomponent self-diffusion technique. *J. Colloid Interface Sci.* 94:463–469.

Stilbs, P. 1987. Fourier transform pulsed field gradient spin-echo studies of molecular diffusion. *Prog. NMR Spectrosc.* 19:1–45.

Tanner, J. E. 1970. Use of the stimulated echo in NMR diffusion studies. *J. Chem. Phys.* 52:2523–2526.

Toma, F., S. Fermandjian, M. Low, and L. Kisfaludy. 1978. A proton NMR investigation of proline-24 *cis-trans* isomerism in corticotropin$_{1-32}$ and related peptides. *Biochim. Biophys. Acta.* 534:112–122.

Toma, F., S. Fermandjian, M. Low, and L. Kisfaludy. 1981. ^{13}C NMR studies of ACTH: assignment of resonances and conformational features. *Biopolymers.* 20:901–913.

Tunga, A., and R. V. Hosur. 1992. Two-dimensional NMR studies on 1–10 fragment of adrenocorticotropic hormone. *Indian J. Biochem. Biophys.* 29:231–235.

Uegaki, K., N. Nemoto, M. Shimizu, T. Wada, Y. Kyogoku, and Y. Kobayashi. 1996. ^{15}N labeling method of peptides using a thioredoxin gene fusion expression system: an application to ACTh (1–24). *FEBS Lett.* 379:47–50.

Wuthrich, K. 1986. NMR of Proteins and Nucleic Acids. John Wiley, New York.